

A BROADBAND GROOVE GUIDE COUPLER FOR MILLIMETER-WAVE APPLICATIONS

Ruediger Vahldieck* and Jim Ruxton**

*Dept. of Electrical Engineering
University of Victoria
P.O. Box 1700
Victoria, B.C., Canada V8W 2Y2

** Bolriet Tech. Inc.
150 Mill St., P.O. Box 53
Carleton Place
Ontario, Canada K7C 3P3

ABSTRACT

In this paper we describe the theoretical design and performance of a broadband groove guide coupler. In contrast to conventional design techniques one of the grooves is partially filled with a dielectric. Both grooves are coupled via a slot in a thin metallic septum separating the grooves. It will be shown how a flat coupling over a wide frequency range can be obtained by taking advantage of the dispersion of even and odd modes and the frequency dependence of the modes in the individual grooves.

INTRODUCTION

The use of conventional rectangular waveguides operating in their fundamental mode at millimeter wave frequencies can cause considerable attenuation, especially at frequencies beyond 100 GHz. Furthermore, the dimensions become very small at those frequencies resulting in manufacturing difficulties. As a possible alternative for some applications, groove guides have been suggested as millimeter wave transmission media featuring the advantage of low losses in this frequency range [1], and relaxed mechanical tolerance requirements due to larger cross-section dimensions. The single groove guide has been proposed as leaky wave antenna, [2]-[3] for example, whereas the double groove configuration can be useful for the design of millimeter wave couplers. The bandwidth of such couplers, however, is normally small to moderate when the groove dimensions are equal. Wider bandwidth have been obtained recently by using asymmetrical groove dimensions [4]. This method was reported to provide flat coupling over a 10 GHz range in the E-band with a measured directivity of better than 40dB.

Since the principle of wideband coupling between asymmetrical lines is not only limited to groove guides, it can also be applied to coupled dielectric slab waveguides (coupled H-guides) or image lines. This was shown

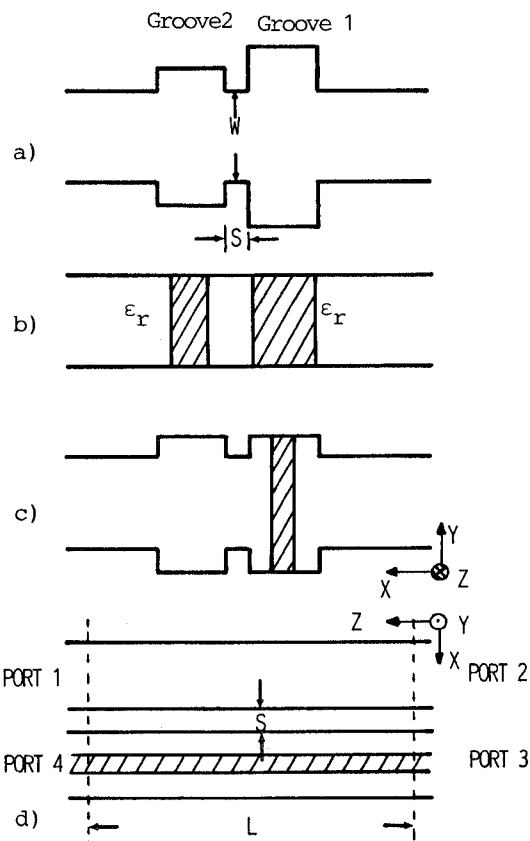


FIG.1 a) cross-section of a groove guide with different groove dimensions; b) coupled H-guide with different slab dimensions; c) double groove guide with partial dielectric loading in groove 1; d) topview of the coupling section in cross-section c).

in [7] for a 3dB H-guide coupler having different slab dimensions.

In this paper we investigate double groove guides having identical groove dimensions but with a partial dielectric loading in one of the grooves. By keeping both groove dimensions constant, the coupler cross-section is

still asymmetrical due to the single dielectric slab. Also this configuration provides a flat coupling over a wide frequency range as shown in Fig. 3. In contrast to the approach in [4], however, we chose the groove separation wall 's' to be fairly thin such that the coupling aperture 'w' (Fig. 1) can be realized very accurately with photolithographic techniques rather than by precision machining as in [4]. This is clearly an advantage because the coupling characteristic over the frequency is very sensitive to the parameters 's' and 'w'. Etching the dimensions of the coupling slot in the groove separation wall, the fabrication of the coupler becomes more accurate.

THEORY

In 1954 Miller [6] had shown that in two lossless, uniformly coupled lines with identical propagation constants, a wave which is incident in one line couples all of its energy to the adjacent line after the length L which is determined by

$$L = \frac{\pi}{K_{ze} - K_{zo}} \quad (1)$$

A 3dB coupling, for example, can be achieved by choosing L accordingly shorter such that only half the energy transfers from one guide to the other. The scattering coefficients $S13$ (input port 1, output port 3, Fig. 1e) is given as a function of the coupling length L .

$$|S13| = \left| \frac{\Delta K}{\sqrt{\Delta K^2 - \Delta k^2}} \cdot \sin\left(\frac{\Delta K}{2} \cdot L\right) \right| \quad (2)$$

$\Delta K = K_{ze} - K_{zo}$, $\Delta k = K_{z1} - K_{z2}$. K_{ze} and K_{zo} are the even and odd modes of the coupled system while K_{z1} , K_{z2} are the propagation constants of the uncoupled,

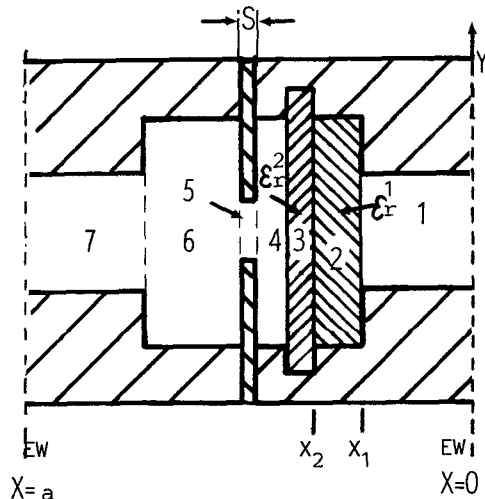


FIG.2 Generalized cross-section of a double groove guide with multi-layered dielectric in one groove.

individual lines. For identical groove dimensions with homogeneous cross-section, $K_{z1} - K_{z2}$ becomes zero and Eqn. (2) reduces to

$$|S13| = \left| \sin\left(\frac{\Delta K}{2} \cdot L\right) \right| \quad (3)$$

However, the bandwidth of such a configuration is relatively small because the difference in the phase constants ΔK decreases rapidly with increasing frequency, thus changing $S13$ significantly. To counteract this tendency we can introduce a dielectric slab in one of the grooves or choose different groove dimensions. Both measures will change the propagation of the individual guides such that they become different. In this case $S13$ must be calculated with Eqn. (2). It can be seen from the equation that we gain a higher degree of freedom in designing a constant output power over the frequency when Δk increases while ΔK decreases, and when the increase of Δk can be manipulated. This is indeed the situation when we insert a dielectric slab in one of the grooves. The value of K_{ze} and K_{zo} will grow with increasing frequency but the difference between them still decreases. In contrast, Δk increases significantly especially when we use a dielectric slab in one of the grooves. The propagation constant in that groove will approach $\sqrt{\epsilon_r}$ for an infinite frequency while the one in the empty groove will approach 1. The dispersion effect on K_{ze} and K_{zo} as well as K_{z1} and K_{z2} is shown in Fig. 4. From this figure and Eqn. (2) it becomes clear that for a proper choice of dimensions the value of Δk over the frequency can compensate for the decreasing tendency of ΔK . Indeed, the numerical calculation of even and odd modes in the coupled groove guide with inhomogeneous cross-section requires a greater effort compared with that of the homogeneous cross-section. Due to the dielectric loading the modes are neither purely TE - nor TM -types but rather a combination, namely hybrid modes. These modes have been calculated using a hybrid mode analysis [5] which was modified and applied to the generalized groove guide structure shown in Fig. 2.

The electromagnetic field in each homogeneous subregion

$$\vec{E} = \nabla X \nabla X A_{ez} \cdot \vec{z} - jw_\mu \nabla X A_{mz} \cdot \vec{z} \quad (4)$$

$$\vec{H} = \nabla X \nabla X A_{mz} \cdot \vec{z} + jw_\epsilon \nabla X A_{ez} \cdot \vec{z} \quad (5)$$

can be derived from the potential functions A_{mz} and A_{ez} which are sums over orthogonal eigenfunctions defined in each subregion as:

$$A_{mz} = \sum_n \frac{\cos(Ky_n \cdot Y)}{\sqrt{1 + \delta \alpha_n}} \cdot I m_n(x) e^{-j k z z} \\ A_{ez} = \sum_n \sin(Ky_n \cdot Y) U e_n(x) e^{-j k z z} \quad (6)$$

Matching the tangential field components E_y , E_z , H_y

and H_z at the common interfaces between subregions leads to a matrix which relates the complex wave amplitudes \underline{I} and \underline{U} of the adjacent subregions to each other (for example at interface x_1 , Fig. 2)

$$\left[\begin{array}{c} \underline{U}^{(2)} \\ \underline{I}^{(2)} \end{array} \right]_{z=x_1} = (\underline{Y}) \left[\begin{array}{c} \underline{U}^{(1)} \\ \underline{I}^{(1)} \end{array} \right]_{z=x_1} \quad (7)$$

At the interfaces within a homogeneous subregion these wave amplitudes are related by a simple transmission line matrix containing only diagonal submatrices with sinusoidal elements.

$$\left[\begin{array}{c} \underline{U}^{(2)} \\ \underline{I}^{(2)} \end{array} \right]_{z=x_2} = \underbrace{\left(\begin{array}{cc} \underline{R}_c & \underline{R}_s \\ \underline{R}_s' & \underline{R}_c \end{array} \right)}_{R^{(2)}} \left[\begin{array}{c} \underline{U}^{(2)} \\ \underline{I}^{(2)} \end{array} \right]_{z=x_1} \quad (8)$$

For details of this procedure the reader is referred to [5]. The advantage of this method is that an arbitrary number of different subregions (which can be different in its y-dimensions and dielectric constant) can be combined by simply multiplying the corresponding matrices according to the sequence of their occurrence. For the example in Fig. 2 this leads to the following matrix equation system

$$\left[\begin{array}{c} \underline{U}^{(7)} \\ \underline{I}^{(7)} \end{array} \right]_{z=a} = \underbrace{\underline{R}^{(7)} \prod_{\nu=1}^6 \underline{Y}^{(\nu)} \underline{R}^{(\nu)}}_{R^{(7)}} \left[\begin{array}{c} \underline{U}^{(1)} \\ \underline{I}^{(1)} \end{array} \right]_{z=0} \quad (9)$$

The boundary conditions in x-direction are satisfied by considering electric walls which are placed far enough away from the groove section. Since \underline{U} is proportional to E_y and E_z (which are zero at an electric wall) the homogeneous matrix equation reduces to the upper right quarter of the matrix product Eqn. (9)

$$\underline{Q} = \underline{G} \underline{I}^{(1)} \quad (10)$$

Eqn. (10) must then be solved for the unknown propagation constant K_z/ko .

RESULTS

Fig. 3 shows the theoretical performance of the prototype coupler with an average of 3.5dB attenuation over a frequency range of 25 GHz. For comparison a symmetrical groove guide coupler in the same frequency range shows a constant increase in attenuation from 1.5dB at 60 GHz up to 4.2 dB at 85 GHz. At frequencies higher than 85 GHz the performance of the new design deteriorates rapidly because then the difference between the propagation constants of the individual grooves Δk become predominant in Eqn. (2). This can also be seen from the dispersion diagram in Fig. 4. The propagation constant of groove 1 containing the dielectric slab approaches $\sqrt{\epsilon_r}$ for infinite frequency while the propagation constant of groove 2 approaches 1. Even and odd modes of the coupled system however, are both approaching $\sqrt{\epsilon_r}$ and the difference ΔK becomes very

small compared to Δk . The frequency behaviour of K_{ze} , K_{zo} and K_{z1} and K_{z2} can be adjusted by changing the structural parameters of the cross-section. For a given substrate thickness and relative permittivity, Fig. 5 shows the influence of the groove separation 's' on even and odd modes. As expected, for small 's' the difference between both modes increases while the slot width 'w' affects only the even mode cutoff frequency as shown in Fig. 6. For two reasons a small groove separation is very interesting for the practical realization of groove guide couplers: Firstly, the even mode is more sensitive to variations in the slot width 'w', which offers the possibility to manipulate the difference between even and odd modes simply by changing 'w'. Secondly, if 's' remains smaller than 200. μm then the slot in the groove separation wall 'w' can be fabricated by photolithographic technique rather than by precision machining.

Also shown in Fig. 6 is the variation in the cutoff frequency for both modes when the height of groove 2 changes. Again, only the HE_{even} -mode (HE_e) is affected while the HE_{odd} -mode (HE_o) remains constant. This result is easy to understand since the HE_o -mode is essentially the fundamental mode of the single groove guide and is therefore virtually not affected when we change the dimensions of only one groove. In contrast, the HE_e -mode exist as the first higher order mode in the double groove guide and consequently depends very much on the dimensions of both grooves.

CONCLUSION

The design of a wideband groove guide coupler, partially loaded with a thin dielectric, has been introduced. Due to the dielectric material in one of the grooves the coupler shows a constant coupling between 60 GHz to 85 GHz. Utilizing a thin metallic sheet to separate the grooves, photolithographic techniques can be used to fabricate the coupling aperture in the septum. This measure simplifies the mechanical design and makes it more accurate.

REFERENCES

1. D.J. Harris, K.W. Lee, "Characteristics of Double Groove Guide at 3 mm Wavelength", Electronic Letters, Vol. 14, No. 23 pp. 726-727, Nov. 9, 1978.
2. A.A. Oliner and P. Lampariello, "A Novel Leaky-Wave Antenna for Millimeter-Waves", Electronic Letters, Vol. 18, No 25/26, pp. 1105-1106, Dec. 9, 1982.
3. P. Lampariello and A.A. Oliner, "Theory and Design Considerations for Millimeter-Wave Leaky Groove Guide Antenna", Electronic Letters, Vol 19, No. 1., pp. 18-20, Jan. 6, 1983.

4. J. Meissner, "Groove-Guide Directional Couplers with Improved Bandwidth", *Electronic Letters*, Vol. 20, No. 17, pp. 701-703, Aug. 16, 1984.

5. R. Vahldieck, "Accurate Hybrid Mode Analysis of Various Finline Configuration Including Multilayered Dielectrics, Finite Metallization Thickness and Substrate Holding Grooves", *IEEE Trans. MTT-32*, pp. 1445-1460, Nov. 1984.

6. S.E. Miller, "Coupled Wave Theory and Waveguide Applications", *Bell Syst. Techn. Journal*, 33, pp. 661-719, 1954.

7. P.K. Ikkäläinen, G.L. Matthaei and M.M. Monte, "Broadband Waveguide 3-dB Couplers Using Asymmetrical Coupled Lines", *IEEE MTT-S*, pp.135-148, 1986.

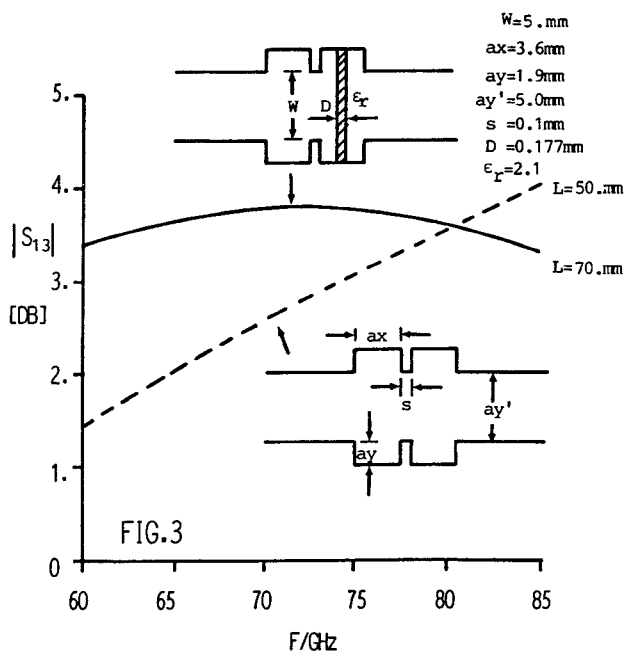


FIG.4 Dispersion diagram for even and odd modes in a partially dielectric loaded groove guide (—). Dotted lines show the dispersion of the fundamental mode in a single groove guide with dielectric loading (-----) and with homogeneous cross-section (---).

FIG.5 Even and odd mode propagation constants versus the groove separation 's'

FIG.6 Cutoff frequencies of even HE_e and odd modes HE_o versus the groove height in groove 2 and versus the slot width 'W'.

